

# Face-elicited ERPs and affective attitude: brain electric microstate and tomography analyses

D. Pizzagalli<sup>a,b,\*</sup>, D. Lehmann<sup>a,b</sup>, T. Koenig<sup>b</sup>, M. REGARD<sup>a</sup>, R.D. Pascual-Marqui<sup>b</sup>

<sup>a</sup>Department of Neurology, University Hospital, CH-8091 Zurich, Switzerland

<sup>b</sup>The KEY Institute for Brain-Mind Research, University Hospital of Psychiatry, CH-8029 Zurich, Switzerland

Accepted 20 September 1999

## Abstract

**Objectives:** Although behavioral studies have demonstrated that normative affective traits modulate the processing of facial and emotionally charged stimuli, direct electrophysiological evidence for this modulation is still lacking.

**Methods:** Event-related potential (ERP) data associated with personal, traitlike approach- or withdrawal-related attitude (assessed post-recording and 14 months later) were investigated in 18 subjects during task-free (i.e. unrequested, spontaneous) emotional evaluation of faces. Temporal and spatial aspects of 27 channel ERP were analyzed with microstate analysis and low resolution electromagnetic tomography (LORETA), a new method to compute 3 dimensional cortical current density implemented in the Talairach brain atlas.

**Results:** Microstate analysis showed group differences 132–196 and 196–272 ms poststimulus, with right-shifted electric gravity centers for subjects with negative affective attitude. During these (over subjects reliably identifiable) personality-modulated, face-elicited microstates, LORETA revealed activation of bilateral occipito-temporal regions, reportedly associated with facial configuration extraction processes. Negative compared to positive affective attitude showed higher activity right temporal; positive compared to negative attitude showed higher activity left temporo-parieto-occipital.

**Conclusions:** These temporal and spatial aspects suggest that the subject groups differed in brain activity at early, automatic, stimulus-related face processing steps when structural face encoding (configuration extraction) occurs. In sum, the brain functional microstates associated with affect-related personality features modulate brain mechanisms during face processing already at early information processing stages. © 2000 Elsevier Science Ireland Ltd. All rights reserved.

**Keywords:** Emotion; Event related potential microstates; Brain functional imaging; Low resolution electromagnetic tomography; Personality; Laterality

## 1. Introduction

Neuroscientific investigations of face processing identified the occipito-temporal pathway (or ‘ventral stream’) as crucially involved in face identification. Functional magnetic resonance imaging (fMRI; Puce et al., 1995; Kanwisher et al., 1997, 1999; Aguirre et al., 1999), positron emission tomography (PET; Sergent et al., 1992; Haxby et al., 1994) and intracerebral recordings (Allison et al., 1994; Halgren et al., 1994) demonstrated that maximal activation within this pathway is task-dependent and hierarchically organized from posterior to anterior regions. Whereas structural encoding typically activates posterior regions (e.g. posterior fusiform gyrus), identification of specific faces

or retrieval of semantic knowledge about individuals is associated with activation of more anterior regions (e.g. midfusiform, parahippocampal, and midtemporal gyrus).

Ethologically, faces are crucial channels of social cognition because they have high emotional value, and they permit deciphering the intentions of others (Brothers, 1990). Face recognition may thus indirectly reflect encoding and storage of social acts (Brothers, 1990). As expected, brain electric or magnetic signatures of face recognition occur quickly, 50–200 ms post-stimulus (Allison et al., 1994; Halgren et al., 1994; Bötzel et al., 1995; Jeffreys, 1996; Sams et al., 1997; Seeck et al., 1997; Debruille et al., 1998; Swithenby et al., 1998; Eimer and McCarthy, 1999).

In behavioral studies, processing bias while perceiving emotional information (including faces) was demonstrated in induced or pathological affective states. Depressed subjects displayed processing bias towards emotionally negative information (George et al., 1998); induced

\* Corresponding author. Laboratory for Affective Neuroscience, Department of Psychology, University of Wisconsin-Madison, 1202 W. Johnson Street, Madison, WI 53706, USA. Tel.: +1-608-263-5072; fax: +1-608-265-2875.

E-mail address: dpizzag@psyphw.psych.wisc.edu (D. Pizzagalli)

emotions (e.g. happiness, sadness) influenced information processing accordingly (Halberstadt and Niedenthal, 1997). However, no studies have investigated brain mechanisms during face perception as a function of affect-related personality features of the perceiver.

Combining the 3 issues discussed above, the present study investigates the influence of personal affective attitude (subjects' affective reactivity or style; Goldsmith, 1993; Davidson, 1995) on brain electric field data during face processing. Brain electric field analysis can identify the occurrence times of different brain processes. As physical phenomena, different brain field configurations (map landscapes) must have been caused by different active neuronal populations (Fender, 1987), and in terms of physiology it is reasonable to assume that different active neural populations implement different functions. When examining the temporal development of sequences of momentary maps of potential distributions (landscapes of potentials) on the head surface, a recurrent observation is that these sequences consist of brief epochs of quasi-stable map configurations (landscapes), called microstates, that are concatenated by rapid transitions (e.g. Lehmann and Skrandies, 1984; Lehmann, 1987; Koenig and Lehmann, 1996; Koenig et al., 1998). Thus, brain electric field characteristics change in a stepwise manner rather than steadily, although each step or microstate must consist of the activity of many parallel neuronal processes. The microstates were suggested to be the building blocks of a stepwise information processing in the brain; this was supported by several studies (e.g. Lehmann et al., 1998).

In the present study, temporal brain microstate segmentation (Koenig and Lehmann, 1996; Koenig et al., 1998; Lehmann et al., 1998) together with a new brain electric tomography approach: low resolution electromagnetic tomography (LORETA; Pascual-Marqui et al., 1994, 1999) allowed the assessment of the timing and cortical localization of personality-modulated, face-elicited processes, issues not covered in a previous analysis (Pizzagalli et al., 1998). The present study analyzed 27 channel event-related potential (ERP) fields recorded while subjects (dichotomized for their affective, approaching vs. withdrawing attitude towards faces) passively observed face images without tasks, i.e. during unrequested, automatic, emotional evaluation of faces.

## 2. Materials and methods

### 2.1. Subjects

Eighteen healthy subjects (7 female; mean age: 29.4; range 22–37) with no history of neurological or psychiatric disorders and with normal or corrected-to-normal vision participated after informed, written consent to the study (approved by the Ethics Committee). All subjects were right-handed (Oldfield, 1971).

### 2.2. EEG recordings

Twenty seven channel ERPs were recorded during passive observation of face images in a sound, light and electrically shielded room with an intercom system. ERPs were recorded from 27 electrodes (Fpz as recording reference, Fp1/2, Fz, F3/4, F7/8, FC1/2, Cz, C3/4, T7/8, CP1/2, Pz, P3/4, P7/8, PO3/4, Oz and O1/O2) of the 10/10 system (American Electroencephalographic Society, 1991; filter: 0.3–70 Hz; sampling: 256Hz; electrode impedances <5 k $\Omega$ ). Eye movements were recorded from outer left canthus vs. Fpz.

### 2.3. Face images and presentation

Face images were 32 black and white photographic portraits of psychiatric patients ('Szondi-portraits'), particularly suited to evoke emotional decisions (Regard and Landis, 1986). Subjects were naïve to the images to minimize post-perceptual semantic processing, and were instructed to look passively at the face images. The size-, contrast- and brightness-adjusted faces (size: 8 × 11 cm) were presented binocularly, centered in a continually visible frame (size: 18.8 × 12.5 cm) on light gray background on a computer screen (exposure: 450 ms at intervals of 2000 ms; distance: 100 cm). The presentation of the 32 faces was repeated 20 times in newly randomized sequence (1 min intervals).

### 2.4. Affective face ratings and subject group dichotomization

After recording, subjects rated each face image for its affective appeal (liking or disliking) on a vertical 10 cm scale, whose upper and lower ends were labeled 'liked face' and 'disliked face', respectively, or vice versa (constant for given faces). Each face, together with a vertical scale, was presented on an individual hard-copy. Order of rating presentation was randomized over subjects. For each subject, affective attitude was operationalized as mean affective rating of all face images. Subjects were dichotomized into two groups: the 9 subjects with the lowest mean ratings ('general negative affective attitude'; mean = 3.89, SD = 0.89, range: 1.68–4.59), and the 9 subjects with the highest mean ratings ('general positive affective attitude'; mean = 5.34, SD = 0.36, range: 4.72–5.83). The groups did not differ in age, sex, and laterality index (Oldfield, 1971).

### 2.5. Data and statistical analyses

Off-line, all data epochs were reviewed for eye, body movement or other artifacts. After artifact rejection, the ERP map series covering 1024 ms post-stimulus were averaged for each subject using all 32 stimuli and all 20 sequence repetitions, and subsequently recomputed off-line to average reference (digital 1.5–30 Hz temporal band-

pass). A grand mean ERP map series was computed across all subjects.

### 2.5.1. Microstate analysis

In order to identify the start and end time points of the brain electric microstates, relevant changes of the landscape of the momentary potential maps must be detected in the sequence of maps. In the present approach, the map landscapes are assessed by the locations of map descriptors, e.g. the locations of the centroids of the areas of positive and negative potential in the map (Wackermann et al., 1993). In the first map of a sequence, spatial windows are erected around the descriptors. If in a subsequent map a descriptor falls outside of a window, a microstate end is recognized, and a new one starts; the spatial windows are shifted to accommodate the next map's descriptors. Originally, predetermined window sizes were used (Lehmann and Skrandies, 1984; Lehmann, 1987). In the present study, a data-driven approach is used so that window size preselection is avoided (Koenig and Lehmann, 1996; Koenig et al., 1998). This approach involves three basic steps. First, increasing window sizes in steps of 0.01 electrode distance are applied to the map sequence until no more microstate end points are found. Second, the total number of end points across all window sizes is determined for each moment in time, resulting in a probability function of microstate end points. Third, a cut-off level for this function is determined that equally satisfies two goals, stability (i.e. assignment of a maximal number of maps to a given microstate; operationalized as the number of time points where microstate end probability function is smaller than cut-off), and discrimination (i.e. detection of a maximal number of different microstates; operationalized as number of peaks of the end probability function above cut-off). Time points with an end probability above cut-off are accepted as moments of relevant change of map landscape (i.e. as microstate start/end time points). This procedure was applied to the grand mean ERP map series.

For each subject, landscapes were averaged between the identified microstate start and end times; the landscape of each microstate was then reduced to the location of the point of gravity of all absolute voltages (Pizzagalli et al., 1998). As displayed in Fig. 1, this electric gravity center is a conservative estimate of the mean localization of all active, brain electric sources projected orthogonally onto the scalp surface. For each microstate, a global test using a two-dimensional vector analysis approach assessed group differences between gravity centers. This approach treats differences of electric gravity center location between subject groups as two-dimensional vectors, and consists of 3 steps. First, the electric gravity center location of the two subject groups was separately averaged; then the mean difference vector between the two groups was calculated. Finally, the electric gravity center of each subject was projected onto the difference vector, and these positions were compared between attitudes using an unpaired *t* test. Post hoc unpaired *t* tests assessed group differences along

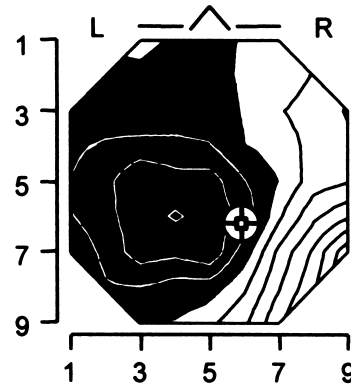


Fig. 1. Spatial feature extraction from a momentary scalp field map. Numbers correspond to the electrode positions of the international 10–10 system as columns (horizontal, left (L) = 1, center = Cz = 5, right (R) = 9) and as rows (vertical, anterior = 1, center = Cz = 5, posterior = 9). The head is seen from above, nose up, left ear left. The cross shows the location of the electric gravity center (point of gravity of the absolute map voltages), indicating the orthogonally underlying location of the mean of all momentarily active processes that produced the measured scalp potential map. Equipotential lines are linearly interpolated in steps of 1  $\mu$ V (black = negative areas, white = positive areas vs. average reference).

the left–right and anterior–posterior brain axis. Overall, two-tailed *P* values are reported.

Only microstates showing significant attitude-dependent differences were further analyzed.

To assess the variance of microstate timing across subjects, microstate start and end times were determined for each subject by computing spatial correlations between the individual map at each time frame and the averaged ('model') microstate maps from the grand mean ERP map series (Brandeis et al., 1992). This individual microstate time recognition used time windows larger than the conventional durations of given components. For example, to assess the individual start and end times for microstate #2, a time window including microstates #1–#4 was used; for microstate #3, microstates #2–#5 were included. For microstate #2, four correlations were computed for each time frame, i.e. between the individual map at that time frame and the model map of microstate #1–#4. The highest correlation assigned each individual map to a specific microstate; the start and end times of the assignments defined the individual microstate start and end times for each subject.

It was further explored whether these assignments were statistically supported, i.e. whether the highest correlations were also significantly different from the other three. For each subject, the averaged map between the individual microstate start and end time was computed; then, 3 *t* values were computed between the highest correlation and the other three using the formula described by Steiger (1980). This procedure allows to test whether the correlation between A (i.e. a specific individual map) and B (i.e. the model map of microstate B) is significantly different from the correlation between A and C (the model map of microstate C), presupposing that the correlation between B and C

is also known. Bonferroni corrected  $P$  values are reported ( $P < 0.017$ ).

### 2.5.2. Brain electric tomography

For the relevant microstates, LORETA (Pascual-Marqui et al., 1994, 1999) computed the three-dimensional intracerebral distributions of current density. The method does not assume a specific number of sources, but solves the inverse problem by computing the ‘smoothest’ of all possible activity distributions (i.e. assuming related orientations and strengths of neighboring neuronal sources). The assumption of simultaneous and synchronous activation of neighboring neurons is supported by animal single unit recordings (Llinas, 1988; Kreiter and Singer, 1992; Haalman and Vaadia, 1997). At each voxel, LORETA computes current density as the linear, weighted sum of the scalp electric potentials. Previous studies employing LORETA showed that the method is able to provide physiologically meaningful results, e.g. during basic visual and auditory tasks (Pascual-Marqui et al., 1994), epileptic discharges (Lantz et al., 1997), as well as cognitive tasks known to engage specific brain regions as assessed with other imaging techniques (Brandeis et al., 1998; Strik et al., 1998).

The utilized LORETA version (Pascual-Marqui et al., 1999) was registered to the Talairach brain atlas (Talairach and Tournoux, 1988), and computations were restricted to cortical gray matter and hippocampus (using the digitized Talairach and probability atlases of the Brain Imaging Centre, Montreal Neurologic Institute). The solution space consisted of 2394 voxels with a spatial resolution of 7 mm. For microstates with significant differences between groups, two average LORETA images were constructed across subjects: the brain electric activity during the microstates, and the voxel-by-voxel  $t$  test differences between groups. The Structure-Probability Maps atlas (Lancaster et al., 1997) was used to assess which brain regions were involved in personality-modulated microstate as well as in differences between the subject groups: Brodmann area(s) and brain regions closest to the observed locations identified by the Talairach coordinates are reported.

### 2.6. Test–retest reliability of affective attitude as trait

The 18 subjects were asked by mail 14 months (on the average) after the ERP experiment to rate the same face images again; 14 replied.

## 3. Results

### 3.1. Microstate analysis

In the present data, 9 microstates with different mean topographies (see Table 1, third column) were identified. For each of the 9 grand mean microstates and both subject groups, Table 1 lists the location of the electric gravity center and the vector tested for group differences. The grav-

ity centers differed significantly between groups in microstates #2 (132–196 ms;  $t = 3.46$ , d.f. = 16;  $P < 0.003$ ) and #3 (196–272 ms;  $t = 2.38$ , d.f. = 16;  $P < 0.03$ ). Post hoc testing revealed that the electric gravity center for subjects with negative affective attitude was significantly more to the right than for subjects with positive attitude in both microstates (both  $t = 2.38$ , d.f. = 16;  $P < 0.03$ ). Anterior–posterior differences were not significant.

As shown in Table 1, microstate #2 had a posterior negative landscape, #3 a posterior positive landscape, both with strongest gradients over occipital areas. Beyond polarity, and across subjects, the landscape of microstates #2 and #3 assessed by the electric gravity center differed in a global test (vector analysis approach) at  $P < 0.028$  ( $t = 2.41$ , d.f. = 16); post hoc testing showed that microstate #2’s electric gravity center was more posterior ( $t = 2.16$ , d.f. = 16;  $P < 0.046$ ).

Fig. 2 displays the locations of the electric gravity centers for the two subject groups for all 9 microstates. This allows

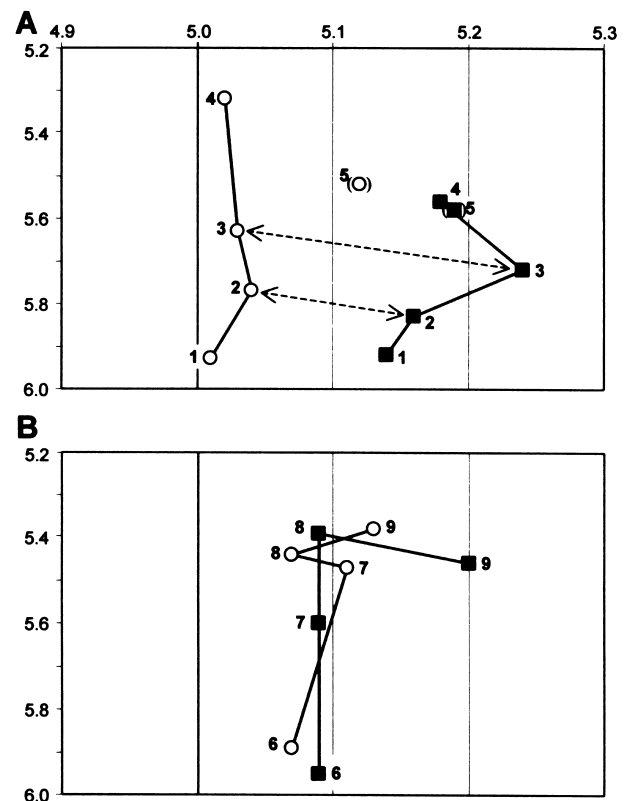
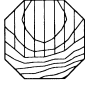
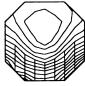
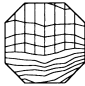
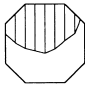
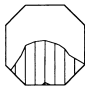
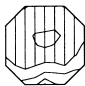
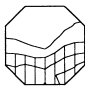
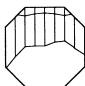
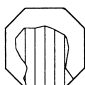


Fig. 2. Mean locations of the brain's electric gravity centers of the nine identified microstates for subjects with negative ( $n = 9$ ; ■) and for subjects with positive ( $n = 9$ ; ○) affective attitude. The frames (head seen from above, anterior is up) display an area near the vertex, around the sagittal midline (heavy vertical line at 5.0), extending from electrode position 4.9 to 5.3 on the left–right axis ( $x$  axis) and from position 5.2–6.0 on the anterior–posterior axis ( $y$  axis), using the position numbering of Fig. 1. Dashed arrows display significant group differences. (A) Locations of the electric gravity centers for the microstates #1–#5. (B) Locations of the electric gravity centers for microstates #6–#9. The location of microstate #5 (332–576 ms) is in brackets because it straddled the end of the stimulus exposure, which occurred at 450 ms.

Table 1

Mean locations (and SD) of the electric gravity centers on the left–right (L-R) and anterior–posterior (A-P) axes of the head in the 9 identified microstates, for subjects with negative ( $n=9$ ) and with positive ( $n=9$ ) affective attitude. The locations are the electrode positions as in Fig. 1. Equipotential lines are linearly interpolated in steps of  $1 \mu\text{V}$  (vertical hatching = negative areas, white = positive areas vs. average reference). Group differences were assessed as two-dimensional vectors. Two-tailed  $P$  values are reported

No.	Microstate		Affective attitude			Vector	$P$ value	
	Timing (ms)	Topography	Negative	Positive	Difference			
#1	80–132		L-R	5.14 (0.14)	5.01 (0.20)	0.126	0.126	0.138
			A-P	5.92 (0.15)	5.93 (0.18)	-0.010		
#2	132–196		L-R	5.16 (0.11)	5.04 (0.10)	0.120	0.134	0.003
			A-P	5.83 (0.19)	5.77 (0.18)	0.059		
#3	196–272		L-R	5.24 (0.13)	5.03 (0.22)	0.204	0.224	0.030
			A-P	5.72 (0.18)	5.63 (0.31)	0.092		
#4	272–332		L-R	5.18 (0.20)	5.02 (0.25)	0.156	0.284	0.096
			A-P	5.56 (0.39)	5.32 (0.26)	0.237		
#5	332–576		L-R	5.19 (0.22)	5.12 (0.13)	0.066	0.092	0.318
			A-P	5.58 (0.11)	5.52 (0.32)	0.064		
#6	576–616		L-R	5.09 (0.19)	5.07 (0.23)	0.022	0.065	0.724
			A-P	5.95 (0.43)	5.89 (0.32)	0.061		
#7	616–668		L-R	5.09 (0.13)	5.11 (0.24)	-0.020	0.131	0.280
			A-P	5.60 (0.16)	5.47 (0.29)	0.130		
#8	668–876		L-R	5.09 (0.25)	5.07 (0.11)	0.019	0.058	0.661
			A-P	5.39 (0.20)	5.44 (0.33)	-0.055		
#9	876–948		L-R	5.20 (0.35)	5.13 (0.25)	0.073	0.111	0.516
			A-P	5.46 (0.46)	5.38 (0.31)	0.083		

following how the activity generally developed as well as how the group differences changed in time. Fig. 2A,B shows the locations for the microstates before and after offset of the stimulus presentation (occurring at 450 ms), respectively. Generally, the subject groups clearly differed during stimulus presentation but not after stimulus offset. Moreover, both after stimulus onset and again after stimulus offset, the gravity center was located most posteriorly, and

for the subsequent microstates it moved more anterior (microstate #5 was an exception but its posteriorization is most probably related to the stimulus offset occurring during its time duration).

The start and end times of microstates #2 and #3 were successfully identified with small variance in all subjects. (The time window, where the spatial correlations were computed, was 80–332 ms for microstate #2 and 132–576

ms for microstate #3). Across subjects, the means of the individual start and end times were  $134.2 \pm 8.7$  and  $190.7 \pm 8.7$  ms for microstate #2 (grand mean ERP map series: 132–196 ms), and  $195.3 \pm 8.3$  and  $275.6 \pm 28.2$  ms for microstate #3 (grand mean ERP map series: 196–272 ms). Two additional results were of relevance. First, for each subject, the sequence of the assignments for both microstates was always uninterrupted (i.e. the occurrence of a new assignment unambiguously started the occurrence

of the next microstate). Second, the assignments were not only unambiguous but also very robust, as assessed by testing the differences between dependent correlations (Steiger, 1980). Considering the individual microstate start and end times related to microstate #2, all 18 subjects displayed significantly higher correlations for the model map of microstate #2 than of microstates #1, #3 and #4 (all  $P$  values  $<0.017$ ). Similarly, for microstate #3, 17 of 18 subjects (binomial  $P$  (17/18)  $<0.0001$ ) displayed significantly higher correlations for the model map of microstate #3 than of microstates #2, #4 and #5 (all  $P$  values  $<0.017$ ).

### 3.2. LORETA tomography

The results of the microstate analysis demonstrated that significantly different neural populations were active in the two subject groups during microstates #2 and #3. The LORETA analysis showed that microstates # 2 and #3 were characterized by a bilateral occipito-temporal activation, involving the lingual and fusiform gyri, and extending to the inferior temporal gyri (Brodmann areas 18, 19, 37, 39). Difference tests (Fig. 3 and Table 2) comparing activity between subject groups showed, for subjects with negative attitude, the strongest activity excess in both microstates in right temporal areas (for microstate #2 more inferior than for #3), whereas for subjects with positive attitude, the strongest activity excess occurred in microstate #2 in left temporo-parietal areas and in microstate #3 in left occipital areas.

Besides the voxels with maximal  $t$  values, other voxels showed group differences with a  $P$  value  $<0.05$  (uncorrected for multiple testing). As listed in Table 2, for microstate #2, subjects with negative attitude had stronger activity in the right middle temporal gyrus, right postcentral gyrus, and bilateral cingulate gyri. For microstate #3, subjects with negative attitude had stronger activity in the precentral, inferior temporal and fusiform gyrus as well as in the inferior parietal lobule, all in the right hemisphere.

### 3.3. ERP waveform analysis

In order to compare the present results with those

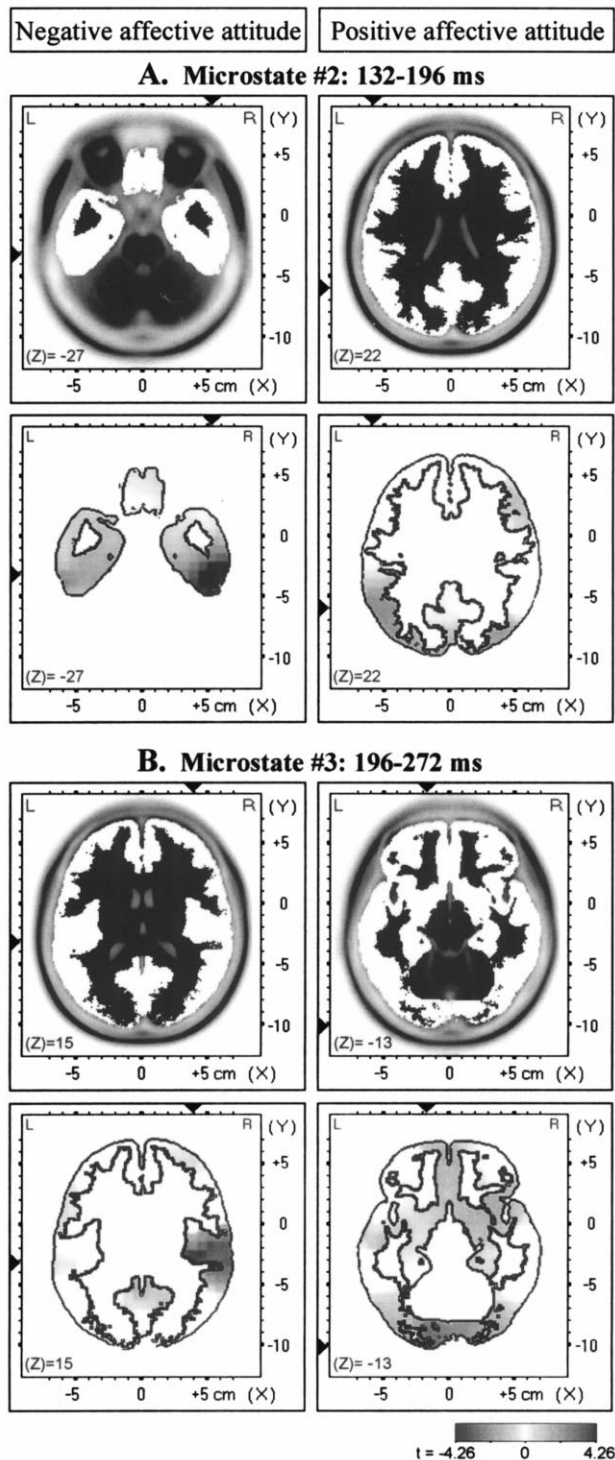


Fig. 3. Images of voxel-by-voxel LORETA  $t$ -statistics of brain electric activity comparing subjects with negative ( $n = 9$ ) and positive ( $n = 9$ ) affective attitude during the microstate #2 (132–196 ms; A) and #3 (196–272 ms; B). Axial brain slices (head seen from above, nose up, L = left, R = right) are shown at the level (indicated as Z-axis values at the lower left corners) of the extreme  $t$  values. In (A) and (B), the upper images show LORETA's cortical solution areas in white; the lower images display the  $t$  values as gray shades (see calibration) in these areas. Locations of extreme  $t$  values (values see Table 2) are indicated by black triangles. Left images show relative hyperactivity for subjects with negative affective attitude; right images show relative hyperactivity for subjects with positive affective attitude. Coordinates in mm after Talairach and Tournoux (1988); origin at anterior commissure; (X) = left (–) to right (+); (Y) = posterior (–) to anterior (+); (Z) = inferior (–) to superior (+). Note that paired upper and lower images are at the same Z-level.

Table 2

Results of the voxel-by-voxels LORETA  $t$  statistics comparing subjects with negative ( $n = 9$ ) and positive ( $n = 9$ ) affective attitude for microstate #2 (132–196 ms) and #3 (196–272 ms). Coordinates in mm after Talairach and Tournoux (1988); origin at anterior commissure; X = left (–) to right (+); Y = posterior (–) to anterior (+); Z = inferior (–) to superior (+). Brodmann areas (BA) and anatomical regions of the extreme  $t$  values<sup>a</sup> and  $t$  values associated with  $P$  values  $< 0.05$  (<sup>b</sup>; uncorrected for multiple testing) are reported (d.f. = 16). Positive  $t$  values indicate relative hyperactivity, negative values relative hypoactivity in subjects with negative affective attitude

Microstate	Affective attitude	X	Y	Z	$t$ value	BA	Region	Side
#2	Negative > positive	53	–32	–27	4.26 <sup>a</sup>	BA 20	Fusiform gyrus	Right
		60	–25	–6	3.79 <sup>b</sup>	BA 21	Middle temporal gyrus	Right
		67	–11	22	2.82 <sup>b</sup>	BA 43	Postcentral gyrus	Right
		11	24	36	2.41 <sup>b</sup>	BA 32	Cingulate gyrus	Right
		–3	24	36	2.38 <sup>b</sup>	BA 32	Cingulate gyrus	Left
	Positive > Negative	46	–25	43	2.15 <sup>b</sup>	BA 2	Postcentral gyrus	Right
		–59	–60	22	–1.84 <sup>a</sup>	BA 44	Superior temporal gyrus	Left
#3	Negative > Positive	39	–32	15	3.39 <sup>a</sup>	BA 29	Superior temporal gyrus	Right
		60	–32	15	2.99 <sup>b</sup>	BA 42	Superior temporal gyrus	Right
		67	–11	29	2.75 <sup>b</sup>	BA 6	Precentral gyrus	Right
		60	–25	–27	2.67 <sup>b</sup>	BA 20	Inferior temporal gyrus	Right
		60	–39	–27	2.54 <sup>b</sup>	BA 20	Fusiform gyrus	Right
		39	–53	43	2.51 <sup>b</sup>	BA 40	Inferior parietal lobule	Right
	Positive > Negative	–17	–102	–13	–2.48 <sup>a</sup>	BA 17	Lingual gyrus	Left

obtained with conventional ERP waveform analyses, average amplitudes were computed (vs. technical zero baseline) for every subject using the individual microstate start and end times of microstates #2 and #3. These values were subjected to analyses of variance (ANOVA) separately for midline (Fpz, Fz, Cz, Pz, Oz), anterior (Fp1/2, F3/4, F7/8, FC1/2), central (C3/4, T7/8, CP1/2) and posterior (P3/4, P7/8, PO3/4, O1/2) electrodes using *Group*, *Electrode* and *Hemisphere* (when appropriate) as factors. Fig. 4 displays the ERP waveshapes separately averaged for subjects with positive and for those with negative affective attitude.

For microstate #2, the only effect approaching significance was a *Group*  $\times$  *Electrode*  $\times$  *Hemisphere* interaction for posterior electrodes ( $F(3, 48) = 2.46$ ;  $P < 0.074$ ). Follow-up analyses showed that this triple interaction was caused by more negative amplitudes at P7 for subjects with positive affective attitude but a reversed pattern at P8 and O2. These results fit well with the left-right group differences demonstrated in the microstate analysis. However, no group differences emerged at single electrodes in the conventional waveshape analysis. The microstate analysis was therefore more sensitive in assessing group differences.

For microstate #3, a significant *Group*  $\times$  *Electrode* interaction emerged ( $F(4, 64) = 3.30$ ;  $P < 0.016$ ) in the ANOVA analysis with midline electrodes: negative affective attitude was associated with more negative amplitude at Fz ( $t = 2.47$ , d.f. = 16;  $P < 0.025$ ) but more positive amplitudes at Oz ( $t = 2.75$ , d.f. = 16;  $P < 0.014$ ). For anterior electrodes, a *Group*  $\times$  *Electrode*  $\times$  *Hemisphere* interaction was found ( $F(3, 48) = 3.17$ ;  $P < 0.032$ ). Follow-up analyses demonstrated group differences at F4 ( $t = 2.44$ , d.f. = 16;  $P < 0.027$ ), F8 ( $t = 2.32$ , d.f. = 16;  $P < 0.034$ ), F3 ( $t = 2.23$ , d.f. = 16;  $P < 0.041$ ), and FC1 ( $t = 2.26$ , d.f. = 16;  $P < 0.038$ ) with larger (more nega-

tive) amplitudes for subjects with negative affective. The main effect of *Group* approached significance ( $F(1, 16) = 3.67$ ;  $P < 0.073$ ). For posterior electrodes, a main effect of *Group* was demonstrated ( $F(1, 16) = 4.59$ ;  $P < 0.048$ ): again, subjects with negative affective attitude had generally higher amplitudes. Significant *Group*  $\times$  *Hemisphere* ( $F(1, 16) = 4.98$ ;  $P < 0.040$ ) and *Group*  $\times$  *Electrode*  $\times$  *Hemisphere* ( $F(3, 48) = 6.33$ ;  $P < 0.001$ ) interactions modulated this effect. Follow-up analyses for the *Group*  $\times$  *Hemisphere* interaction showed that subjects with negative affective attitude had larger amplitudes at electrodes over the right than left hemisphere ( $2.38 \pm 0.77$  vs.  $1.91 \pm 0.63$ ;  $t = 1.93$ , d.f. = 8;  $P < 0.089$ ), and differed from subjects with positive affective attitude only at electrodes over the right hemisphere ( $2.38 \pm 0.77$  vs.  $1.66 \pm 0.67$ ;  $t = 2.11$ , d.f. = 16;  $P < 0.05$ ). Group differences were only found at P8 ( $t = 2.07$ , d.f. = 16;  $P < 0.055$ ), O2 ( $t = 2.67$ , d.f. = 16;  $P < 0.017$ ) and PO4 ( $t = 2.15$ , d.f. = 16;  $P < 0.048$ ). For central electrodes, no significant effects emerged.

#### 3.4. Test-retest reliability of affective attitude as trait

Re-rating of the face images by the same subjects showed that repeat (on the average 416 days after the experiment) and original affective attitudes correlated with Spearman's  $\rho = 0.61$  ( $n = 14$ ,  $P < 0.02$ ).

## 4. Discussion

### 4.1. Temporal aspects of the personality-modulated, face-elicited ERP microstates

The space-oriented microstate analysis employed in the

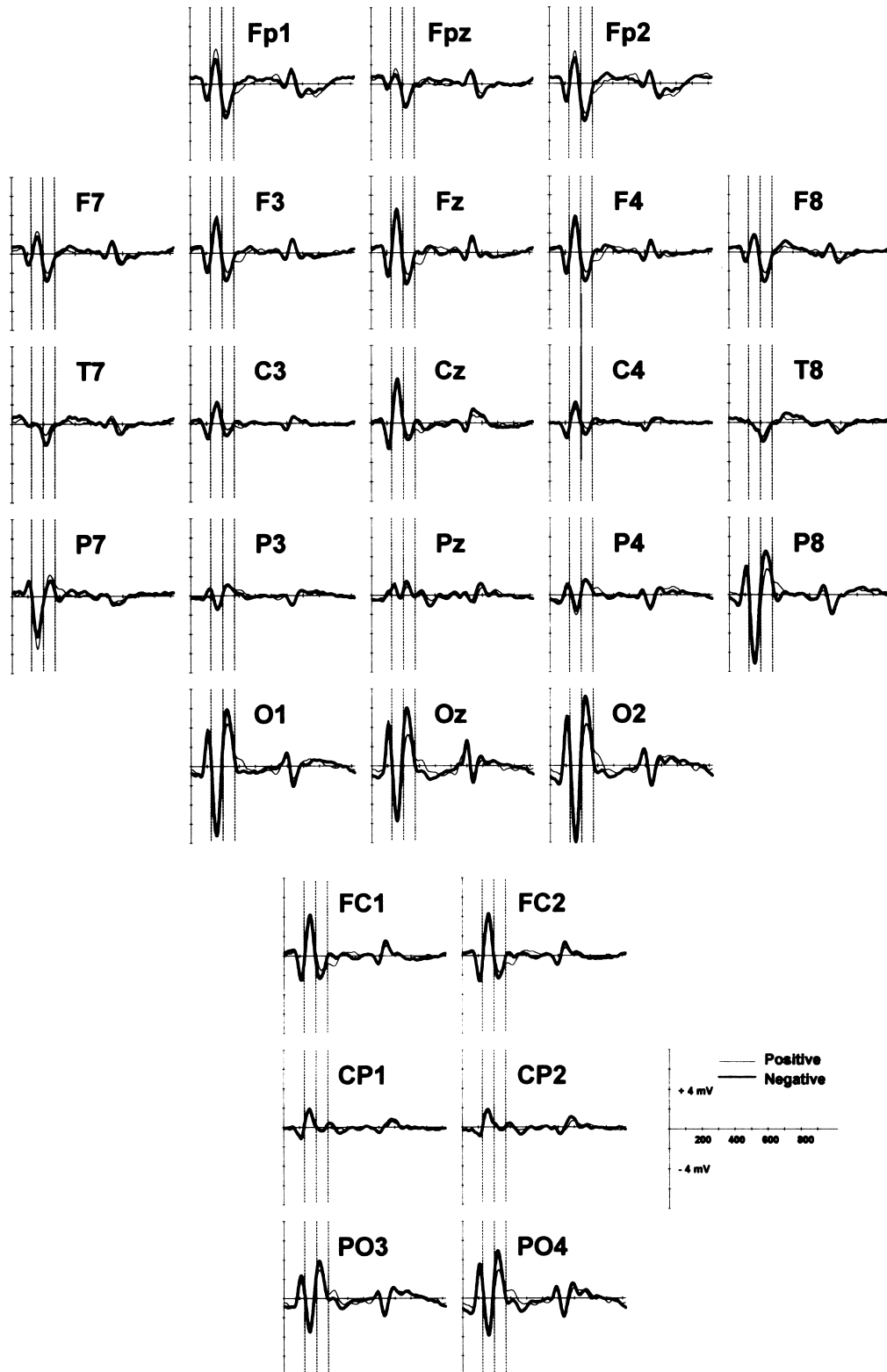


Fig. 4. Mean ERP waveshapes (vs. average reference) separately averaged for subjects with negative affective attitude ( $n = 9$ ; heavy lines) and for subjects with positive affective attitude ( $n = 9$ ; thin lines). The vertical dashed lines illustrate the start and end times for the microstates showing significant group differences in the microstate analysis (microstate #2: 132–196 ms; microstate #3: 196–272 ms). Note that plotting of ERPs at different electrode positions cannot be easily interpreted in terms of the spatial configuration of a momentary field map. Electrode nomenclature according to the international 10–10 system.



present study allowed the discrimination of sequential brain microstates as basic elements of brain information processing (Koenig and Lehmann, 1996; Koenig et al., 1998; Lehmann et al., 1998). The two microstates at 132–196 ms and at 196–272 ms after stimulus onset were systematically influenced by the subjects' affective attitude towards the face images (assessed after the experiment). The timing of these microstates was consistent over subjects (i.e. identifiable unambiguously and reliably in all subjects). During both microstates, the electric gravity center for subjects with negative affective attitude was located more to the right compared to subjects with positive affective attitude. Evidently, different, attitude-dependent neuronal populations were active in the two microstates between 132 and 272 ms after stimulus onset during the passive, task-free observation of faces.

#### 4.2. Spatial aspects of the personality-modulated, face-elicited ERP microstates

During the two personality-modulated microstates, the 3 dimensional distribution of neuronal electrical activity in the brain as computed with LORETA tomography (Pascual-Marqui et al., 1994, 1999) showed maximal differences between groups as follows: stronger activity at right temporal regions for negative affective attitude in both microstates (however, clearly more inferior in microstate #2 than #3), and stronger activity at left temporo-parietal (in microstate #2) or left occipital (in microstate #3) regions for positive attitude. The relative right temporal hyperactivity associated with negative affective attitude agrees with other studies demonstrating involvement of this region in negative, withdrawal-related emotions, such as disgust (Davidson et al., 1990), aversive conditioning (Hugdahl et al., 1995), anticipatory anxiety and predisposition to panic attack (Reiman, 1997) and processing of negatively loaded films (Lane et al., 1997). The relative left temporo-parietal hyperactivity associated with positive affective attitude parallels recent reports of left-sided activation during positive emotion (fronto-temporal junction during assessment of face attractiveness: Nakamura et al., 1998) as well as left-sided inhibition during negative emotion (left temporo-occipital junction during aversive conditioning: Hugdahl et al., 1995). Taken together, the group differences at the scalp (in both the space-oriented and conventional ERP waveform analysis) and in the brain agree with differential hemispheric involvement in emotions (Regard and Landis, 1986; Canli et al., 1998; see Silberman and Weingartner, 1986; Davidson, 1995 for reviews), i.e. with relatively greater involvement of the right (left) hemisphere during negative (positive) emotions. Thus, the automatically generated, differential geometry of brain activity in the present subjects would account for their varying, affective post-hoc rating of the face pictures. These phasic responses may well arise, however, from a background of tonic differences between the subject groups. Indeed, subjects with the (high-

est) positive and negative affective attitude were found to differ already in their baseline EEG activity (i.e. recorded before any stimulus exposure; Pizzagalli et al., 1999). Relevant to the present results, a negative attitude was associated with a right-lateralized intracerebral model source for the EEG beta frequency band.

#### 4.3. Functional significance of the personality-modulated microstates

The first microstate (132–196 ms) with group differences had maximal activity at 160 ms, which parallels latencies of face-sensitive brain activity measured with scalp ERP's (Bötzel et al., 1995; Jeffreys, 1996; Eimer and McCarthy, 1999), depth ERP's (Allison et al., 1994; Halgren et al., 1994) and magnetoencephalogram (Sams et al., 1997; Swithenby et al., 1998). These studies consistently found an automatic, stimulus-related stage of face processing (configuration extraction) between 120 and 200 ms post-stimulus. It is intriguing that the personality-modulated brain electric responses to face stimuli differed already at such early configuration extraction stages ('structural encoding stages', see Bruce and Young, 1986). The LORETA analysis supported this by demonstrating an inferior, bilateral occipito-temporal activation, in an area reportedly associated with the structural encoding stage of face processing (see Section 1).

PET and fMRI studies using visual stimuli demonstrated activation of primary and secondary visual areas during emotional processing (Lane et al., 1997; Lang et al., 1998; Morris et al., 1998; Nakamura et al., 1998). This was accounted for by reentrant processes from more anterior structures (e.g. cingulate, amygdala) associated with attention and/or motivation, indexing adaptive significance (Lang et al., 1998). A direct test of this hypothesis confirmed a modulatory role of the amygdala for brain activity in the extrastriate cortex (Morris et al., 1998). Similar reentrant processing linked to affect-related personality features might have been active in the present paradigm. At least in microstate #2, the relative hyperactivity in the right inferior temporal area was suggestively close to limbic structures. In terms of individual differences in emotional reactivity, a close relationship ( $r = 0.75$ ) between activity in the right amygdala and electrodermal responses during extinction of fear conditioning was recently reported (Furmark et al., 1997).

#### 4.4. Possible influences of the imposed task on face-elicited ERPs

Several ERP studies investigating face processing while engaging the subjects in more demanding, cognitive tasks (e.g. semantic matching tasks, or tasks with long-term memory requirements) demonstrated considerably later face-elicited potentials (300–600 ms; Smith and Halgren, 1987; Sommer et al., 1991; Bobes et al., 1994). However, the subjects in the present study had no prior experience

with the face images and they were engaged in a passive viewing condition, where possible influences of explicit identification or memory searches were minimized or absent. Therefore, the latency differences between studies investigating unconstrained, automatic vs. cognitively demanding face processing may be accounted for by the fact that the brain regions implementing ‘more cognitive’ operations are probably activated in later (i.e. more anteriorly located) stages of the face processing flow (Sergent et al., 1992; Halgren et al., 1994). Although not directly tested, this assumption receives partial support from the present findings of a continuous and systematic anteriorization of the brain electric activity after stimulus onset (and offset).

Summarizing, it has been suggested that a face ‘...is immediately and obligatorily transformed into the representation of a person (with dispositions and intentions) before having access to consciousness’ (Brothers, 1990, p. 35). The present results demonstrate that not only the salience (i.e. its behavioral appetitive or aversive significance) or the perceptual features of a face, but also the disposition of the perceiving subject modulate this immediate and obligatory encoding within a sufficiently brief time for the decision to be interactively useful. This is, to our knowledge, the first demonstration that specific, trait-like, affect-related personality features influence face-elicited brain processes, and it raises the intriguing issue of experience-dependent brain plasticity not only in sensory and motor functions but also in higher brain functions such as face perception, emotional processing, and personality.

## Acknowledgements

We thank Drs. B. Heider and C. Röhrenbach for the digitized Szondi face images, Drs. A.C. Evans and P. Neelin for providing the Talairach MRI and probability atlases, Dr. V.L. Towle for useful information about electrode coordinates in realistic head geometry, and Dr. R.J. Davidson for helpful comments on the manuscript. This study was partially supported by grants from the Swiss National Science Foundation (81ZH-52864) and ‘Holderbank’-Stiftung zur Förderung der wissenschaftlichen Fortbildung to D.P.

## References

Aguirre GK, Singh R, D’Esposito M. Stimulus inversion and the responses of face and object-sensitive cortical areas. *NeuroReport* 1999;10:189–194.

Allison T, Ginter H, McCarthy G, Norbe A, Puce A, Luby M, Spencer D. Face recognition in human extrastriate cortex. *J Neurophysiol* 1994;71:821–825.

American Electroencephalographic Society Guidelines for Standard Electrode Position Nomenclature. *J Clin Neurophysiol* 1991;8:200–202.

Bobes MA, Valdés-Sosa M, Olivares E. An ERP study of expectancy violation in face perception. *Brain Cogn* 1994;26:1–22.

Bötzel K, Schulze S, Stodieck SRG. Scalp topography and analysis of

intracerebral sources of face-evoked potentials. *Exp Brain Res* 1995;104:135–143.

Brandeis D, Naylor H, Halliday R, Callaway E, Yano L. Scopolamine effects on visual information processing, attention, and event-related potential map latencies. *Psychophysiology* 1992;29:315–336.

Brandeis D, van Leeuwen TH, Rubia K, Vitacco D, Steger J, Pascual-Marqui RD, Steinhausen HC. Neuroelectric mapping reveals precursor of stop failures in children with attention deficits. *Behav Brain Res* 1998;94:111–125.

Brothers L. The social brain: a project for integrating primate behavior and neurophysiology in a new domain. *Concepts Neurosci* 1990;1:27–51.

Bruce V, Young A. Understanding face recognition. *Br J Psychol* 1986;77:305–327.

Canli T, Desmond JE, Zhao Z, Glover G, Gabrieli JDE. Hemispheric asymmetry for emotional stimuli detected with fMRI. *NeuroReport* 1998;9:3233–3239.

Davidson RJ. Cerebral asymmetry, emotion, and affective style. In: Davidson RJ, Hugdahl K, editors. *Brain asymmetry*, Cambridge: MIT Press, 1995. pp. 361–387.

Davidson RJ, Ekman P, Saron CD, Senulis JA, Friesen WV. Approach/withdrawal and cerebral asymmetry: I. Emotional expression and brain physiology. *J Pers Soc Psychol* 1990;58:330–341.

Debruille JB, Guillem F, Renault B. ERPs and chronometry of face recognition: following-up Seek et al. and George et al. *NeuroReport* 1998;9:3349–3353.

Eimer M, McCarthy RA. Prosopagnosia and structural encoding of faces: evidence from event-related potentials. *NeuroReport* 1999;10:255–259.

Fender DH. Source localization of brain electric activity. In: Gevins AS, Remond A, editors. *Handbook of electroencephalography and clinical neurophysiology: methods of analysis of brain electrical and magnetic signals, revised series, vol. 1*. Amsterdam: Elsevier, 1987. pp. 355–403.

Furmark T, Fischer H, Wik G, Larsson M, Fredrikson M. The amygdala and individual differences in human fear conditioning. *NeuroReport* 1997;8:3957–3960.

George MS, Huggins T, McDermut W, Parekh PI, Rubinow D, Post RM. Abnormal facial emotion recognition in depression: serial testing in an ultra-rapid-cycling patient. *Behav Modif* 1998;22:192–204.

Goldsmith HH. Temperament: variability in developing emotion systems. In: Lewis M, Haviland JM, editors. *Handbook of emotions*, New York: Guilford Press, 1993. pp. 353–364.

Haalman I, Vaadia E. Dynamics of neuronal interactions: relation to behavior, firing rates, and distance between neurons. *Human Brain Map* 1997;5:249–253.

Halberstadt JB, Niedenthal PM. Emotional state and the use of stimulus dimensions in judgment. *J Pers Soc Psychol* 1997;72:1017–1033.

Halgren E, Baudena P, Heit G, Clarke M, Marinkovic K. Spatio-temporal stages in face and word processing: I. Depth recorded potentials in the human occipital and parietal lobes. *J Physiol (Lond)* 1994;88:1–50.

Haxby JV, Horwitz B, Ungerleider LG, Maisog JM, Pietrini P, Grady CL. The functional organization of human extrastriate cortex: a PET-rCBF study of selective attention to faces and locations. *J Neurosci* 1994;14:6336–6353.

Hugdahl K, Berardi A, Thompson WL, Kosslyn SM, Macy R, Baker DP, Alpert NM, LeDoux JE. Brain mechanisms in human classical conditioning: a PET blood flow study. *NeuroReport* 1995;6:1723–1728.

Jeffreys DA. Evoked potential studies of face and object processing. *Vis Cogn* 1996;3:1–38.

Kanwisher N, McDermott J, Chun MM. The fusiform face area: a module in human extrastriate cortex specialized for face perception. *J Neurosci* 1997;17:4302–4311.

Kanwisher N, Stanley D, Harris A. The fusiform face area is selective for faces not animals. *NeuroReport* 1999;10:183–187.

Koenig T, Lehmann D. Microstates in language-related brain potential maps show noun-verb differences. *Brain Lang* 1996;53:169–182.

Koenig T, Kochi K, Lehmann D. Event-related electric microstates of the brain differ between words with visual and abstract meaning. *Electroenceph clin Neurophysiol* 1998;106:535–546.

- Kreiter AK, Singer W. Oscillatory neuronal responses in the visual cortex of the awake macaque monkey. *Eur J Neurosci* 1992;4:369–375.
- Lancaster JL, Rainey LH, Summerlin JL, Freitas CS, Fox PT, Evans AC, Toga AW, Mazziotta JC. Automated labeling of the human brain – a preliminary report on the development and evaluation of a forward-transform method. *Human Brain Map* 1997;5:238–242.
- Lane RD, Reiman EM, Ahern GL, Schwartz GE, Davidson RJ. Neuroanatomical correlates of happiness, sadness, and disgust. *Am J Psychiatry* 1997;154:926–933.
- Lang PJ, Bradley MM, Fitzsimmons JR, Cuthbert BN, Scott JD, Moulder B, Nangia V. Emotional arousal and activation of the visual cortex: an fMRI analysis. *Psychophysiology* 1998;35:199–210.
- Lantz G, Michel CM, Pascual-Marqui RD, Spinelli L, Seeck M, Seri S, Landis T, Rosen I. Extracranial localization of intracranial interictal epileptiform activity using LORETA (low resolution electromagnetic tomography). *Electroenceph clin Neurophysiol* 1997;102:414–422.
- Lehmann D. Principles of spatial analysis. In: Gevins AS, Remond A, editors. *Handbook of electroencephalography and clinical neurophysiology: methods of analysis of brain electrical and magnetic signals, revised series, vol. 1*. Amsterdam: Elsevier, 1987. pp. 309–354.
- Lehmann D, Skrandies W. Spatial analysis of evoked potentials in man. A review. *Progr Neurobiol* 1984;23:227–250.
- Lehmann D, Strik WK, Henggeler B, Koenig T, Koukkou M. Brain electric microstates and momentary conscious mind states as building blocks of spontaneous thinking: I. Visual imagery and abstract thoughts. *Int J Psychophysiol* 1998;29:1–11.
- Llinas RR. The intrinsic electrophysiological properties of mammalian neurons: insights into central nervous system function. *Science* 1988;242:1654–1664.
- Morris JS, Friston KJ, Büchel C, Frith CD, Young AW, Calder AJ, Dolan RJ. A neuromodulatory role for the amygdala in processing emotional facial expressions. *Brain* 1998;121:47–57.
- Nakamura K, Kawashina R, Nagumo S, Ito K, Sugiura M, Kato T, Nakamura A, Hatano K, Kubota K, Fukuda H, Kojima S. Neuroanatomical correlates of the assessment of facial attractiveness. *NeuroReport* 1998;9:753–757.
- Oldfield RC. The assessment and analysis of handedness: the Edinburgh inventory. *Neuropsychologia* 1971;9:97–113.
- Pascual-Marqui RD, Michel CM, Lehmann D. Low resolution electromagnetic tomography: a new method for localizing electrical activity in the brain. *Int J Psychophysiol* 1994;7:49–65.
- Pascual-Marqui RD, Lehmann D, Koenig T, Kochi K, Merlo MCG, Hell D, Koukkou M. Functional imaging in acute, neuroleptic-naive, first-episode, productive schizophrenia. *Psychiatry Res. Neuroimaging* 1999;90:169–179.
- Pizzagalli D, Koenig T, Regard M, Lehmann D. Faces and emotions: brain electric field sources during covert emotional processing. *Neuropsychologia* 1998;36:323–332.
- Pizzagalli D, Koenig T, Regard M, Lehmann D. Affective attitudes to face images associated with intracerebral EEG source location before face viewing. *Cogn Brain Res* 1999;7:371–377.
- Puce A, Allison T, Gore JC, McCarthy G. Face-sensitive regions in human extrastriate cortex studied by functional MRI. *J Neurophysiol* 1995;74:1192–1199.
- Regard M, Landis T. Affective and cognitive decisions on faces in normals. In: Ellis HD, Jeeves MA, Newcombe F, Young A, editors. *Aspects of face processing*. Dordrecht: NATO ASI Series, Martinus Nijhoff, 1986. pp. 363–369.
- Reiman EM. The application of positron emission tomography to the study of normal and pathologic emotions. *J Clin Psychiatry* 1997;58:4–12.
- Sams M, Hietanen JK, Hari R, Ilmoniemi RJ, Lounasmaa OV. Face-specific responses from the human inferior occipito-temporal cortex. *Neuroscience* 1997;77:49–55.
- Seeck M, Michel CM, Mainwaring N, Cosgrove R, Blume H, Ives J, Landis T, Schomer DL. Evidence for rapid face recognition from human scalp and intracranial electrodes. *NeuroReport* 1997;8:2749–2754.
- Sergent J, Ohta S, MacDonald B. Functional neuroanatomy of face and object processing. *Brain* 1992;115:15–36.
- Silberman EK, Weingartner H. Hemispheric lateralization of functions related to emotion. *Brain Cogn* 1986;5:322–353.
- Smith ME, Halgren E. Event-related potentials elicited by familiar and unfamiliar faces. In: Johnson Jr. R, Rohrbaugh JW, Parasuram R, editors. *Current trends in event-related potential research (EEG Supplement, 40)*. Amsterdam: Elsevier, 1987. pp. 422–426.
- Sommer W, Schweinberger SR, Matt J. Human brain potential correlates of face encoding into memory. *Electroenceph clin Neurophysiol* 1991;79:457–463.
- Steiger JH. Tests for comparing elements of a correlation matrix. *Psychol Bull* 1980;87:245–251.
- Strik WK, Fallgatter AJ, Brandeis D, Pascual-Marqui RD. Three-dimensional tomography of event-related potentials during response inhibition: evidence for phasic frontal lobe activation. *Electroenceph clin Neurophysiol* 1998;108:406–413.
- Swithey SJ, Bailey AJ, Bräutigam S, Josephs OE, Jousmäki V, Tesche CD. Neural processing of human faces: a magnetoencephalographic study. *Exp Brain Res* 1998;118:501–510.
- Talairach J, Tournoux P. *Co-planar stereotaxic atlas of the human brain*. Stuttgart: Thième, 1988.
- Wackermann J, Lehmann D, Michel CM, Strik WK. Adaptive segmentation of spontaneous EEG map series into spatially defined microstates. *Int J Psychophysiol* 1993;14:269–283.